Journal of Visualization, Vol. 9, No. 1 (2006)111-119

Experimental Study of Convection in a Model Czochralski Crucible Using Liquid Crystal Thermography

Banerjee, J.*[1], Bharadwaj, R.*[2] and Muralidhar, K.*[1]

*1 Department of Mechanical Engineering, Indian Institute of Technology, Kanpur, 208016, India.
*2 Department of Mechanical Engineering, SUNY Stony Brook, New York, USA.
E-mail: kmurli@iitk.ac.in

Received 13 September 2004
Revised 16 September 2005

Abstract : Steady state temperature distribution in a model Czochralski crucible has been mapped by liquid crystal thermography (LCT). The crucible is a water-filled glass beaker. Water is used as the test fluid because of ease of experimentation, as well as the availability of correct thermo-physical properties. In addition, the Prandtl number of water matches those of molten oxides. A copper cylinder whose diameter is smaller than that of the beaker is placed centrally at the water surface. Convection patterns are set up by applying constant temperature difference between the crucible wall and the cylinder surface, in the temperature range of the liquid crystals. The cylinder is given a fixed rotation, thus creating mixed convection conditions in the test fluid. The LCT images recorded in the present study clearly reveal convective rolls, and the interaction of buoyancy-driven convection in the crucible with cylinder rotation. The resulting temperature distributions match numerical simulation quite well. The pure buoyancy and pure rotation experiments result in axisymmetric temperature fields, while in mixed convection, the field is unsteady and three dimensional.

Keywords : Convection, Buoyancy, Rotation, LCT, Axisymmetry, Numerical model.

1. Introduction

Czochralski crystal growth process is a popular technique for growing electronic and optical crystals from their molten state (Szmyd and Suzuki, 2001). It involves introducing a seed crystal into the melt contained in a crucible, while the seed is pulled with a prescribed velocity. Convection patterns are set up in the crucible owing to a temperature difference as well as crystal rotation. These patterns control the quality of the grown crystal. The Czochralski process is conducted at a high temperature and does not permit convenient observation of the convection patterns. Instead, experiments using model fluids have been performed at temperatures closer to ambient, to simulate melt convection in the Czochralski geometry (Jones, 1983; Mukherjee et al., 1996; Hintz and Schwabe, 2001). Such cold model experiments reveal the complicated interaction of transport mechanisms existing in real Czochralski processes. Mathematical models have also been developed to explore these interactions (Derby and Xiao, 1991; Zhang and Prasad, 1995). These models help in conducting simulation under realistic conditions and optimizing process parameters for the growth of high quality crystals.

Numerical computer codes need to be validated against experimental data. Numerical models that adopt the axisymmetric approximation for velocity and temperature lead to erroneous results

for semiconductor melts such as silicon owing to their low Prandtl number. The axisymmetric approximation for oxide melts such as YAG is expected to have greater validity in view of the higher Prandtl number of such materials (Krishnamurti, 1970). In the present study, experiments have been conducted in a glass beaker containing water with a cooled solid cylinder at its surface, in a geometry that resembles the Czochralski apparatus. The thermal field has been mapped using liquid crystal thermography. The images reveal the pattern of buoyant convection, and conditions under which it is altered by cylinder rotation. The temperature distribution obtained using LCT has been compared against the predictions of an axisymmetric numerical model.

2. Experimental Details

2.1 Apparatus and Instrumentation

The experimental setup consists of a glass beaker, a copper cylinder placed at the top surface of water representing a growing crystal, traversing mechanism to control the motion of the crucible and the cylinder, and instrumentation for visualization of the convection patterns (Fig. 1). To facilitate comparison with numerical simulation, the beaker, representing the Czochralski crucible, is specially made of borosilicate glass, and has a flat base. The copper cylinder plays the role of the growing crystal of the Czochralski process. It is however passive, in the sense that a phase change occurring in the real process is not replicated. The crucible is placed on a platform within a constant temperature bath. The copper cylinder is held by a rod that is in turn connected to a stepper motor. Two constant temperature water baths (Raaga) have been used to maintain distinct temperature boundary conditions along the crucible walls and the copper cylinder. The traversing arrangement allows for careful positioning of the cylinder with respect to the beaker axis as well as the light sheet.

1	Light source box with slit
2	Cylindrical lens
3	Optical bench
4	Constant temperature bath
5	Crucible
6	Copper cylinder
7	Lead screw
8	Color CCD
M	Stepper Motor

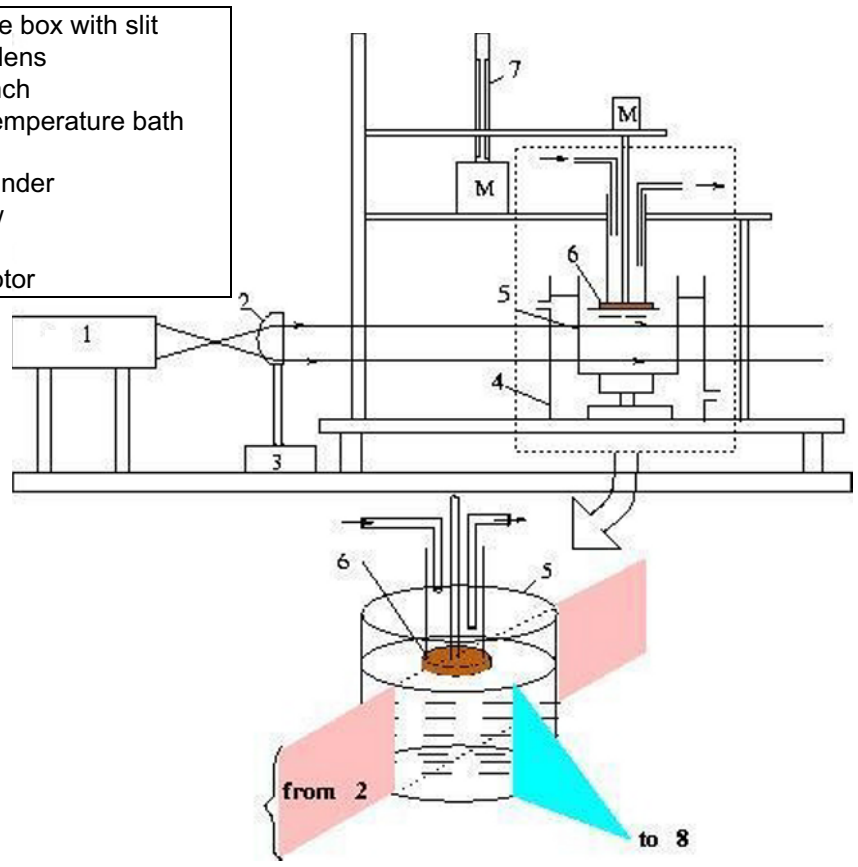

Fig. 1. Schematic diagram of the experimental setup.

Water in the beaker is distilled, de-mineralized, and de-ionized to prevent contamination of the LCT powder, as well as to keep the beaker surface free of deposits. It is mixed with LCT powder (R35C15W, Hallcrest, USA) to provide the nuclei for scattering of light. The LCT specification refers to the activation of the red color at 35°C and a bandwidth of 15°C. The amount of powder added, finalized after several trials, was about 10 grams to half-a-liter of water. Light from a halogen lamp (500 Watts) is passed through a slit and a cylindrical lens to develop a sheet of light in the vertical plane. Light scattered by LCT particles is recorded at normal incidence by a three-color CCD camera.

The image acquisition system used in the present investigation consists of an 8-bit, 512 × 512 resolution color CCD camera (Sony), frame grabber (Basler A201bc) with 25 mm focal length lens (VCL-16WM) and a P-3 PC (HCL, 256MB RAM). These systems store the appropriate intensities of red, green, and blue in the scattered light needed to produce a matched color response corresponding to temperature at each point in the image.

The temperature levels in the experimental setup are much lower than in a real Czochralski set up, but the inter-play of buoyant convection and rotation could be visualized. Typical temperatures realized in the experiment were in the range of 34 to 45°C, the maximum temperature difference applied being 6°C. Rotational speeds of up to 25 rpm were employed. For a beaker diameter of 100 mm and a cylinder diameter of 50 mm, the largest Grashof number Gr was 3.2×10^6, the largest Reynolds number Re of the rotating cylinder being 3.25×10^3. Radius of the crucible is used as the length scale for nondimensionalization (Banerjee and Muralidhar, 2005). The mixed convection parameter, defined as Gr/Re^2, could be varied. Values of the order of unity indicate a strong interaction between the forced and buoyancy-driven flow fields.

Compared to surface thermography, the use of TLC as dilute suspension in a fluid bears additional difficulties in measurement. First, the color images of the flow are discrete as they represent a discontinuous mist of points. Secondly, due to secondary light scattering from particles between the sheet of light and the camera, and its reflections from the sidewalls, the overall color response is distorted. It was seen in the present work that the signal strength, and hence the image quality was good in the central portion of the crucible over 80% of the diameter; it deteriorated in regions near the crucible walls.

2.2 Experimental Procedure

Liquid crystals are uniformly dispersed in water by stirring and introduced in the crucible. The crucible walls and the copper cylinder are maintained at two different temperatures by circulating water individually from constant temperature baths. Sufficient time is allowed to elapse for the flow and thermal fields to stabilize in the beaker. This time period is around one hour for pure buoyancy experiments. Rotation to the copper cylinder is imparted after buoyancy-driven convection is fully established in the beaker. For high rotation rates, a forced convection pattern was seen to be established in around 30 minutes. In the mixed convection regime, a clear steady state was visible only in selected experiments.

For measurements, light from a white light source is passed through a slit and a cylindrical lens to develop a sheet of light in the vertical plane of the crucible. The scattered light is recorded at normal incidence by the CCD camera. All experiments have been conducted in a controlled environment, with temperature and humidity carefully regulated. The ambient temperature during the experiments was maintained in the range of 30 ± 0.2°C. In any particular experiment, the change in the ambient temperature was smaller.

3. Processing of Liquid Crystal Images

To improve the appearance of the convection pattern in the LCT images, the brightness and saturation values were adjusted through a commercially available software package (Irfanview).

The color-to-temperature calibration was based on the hue representation of the components of color. Hence, the hue values were left untouched during the image enhancement operation.

3.1 Hue, Saturation and Intensity (HSI) Color Model

Colors are represented by the tri-stimulus signals, red (R), green (G) and blue (B). These signals can be thought of as outputs from three camera detectors each with its optically sensitive range centered on a different wavelength in the visible spectrum. The RGB representation of color is difficult to use because three values (red, green and blue) may not uniquely interpret the temperature at a point. Additionally, the analytical relationship between the RGB values and temperature is not straightforward. A convenient solution is to use an auxiliary approach based on hue, saturation and intensity (HSI). For commercially available LCT material, hue changes monotonically with temperature and also remains independent of the local illumination strength.

In the present study, the RGB output of the camera has been calibrated against temperature via the hue function. Various relationships permit the calculation of hue from the RGB components of the digitized image. The one described by Ireland and Jones (2000) has been used in the present work. The range of hue is measured as an angle, from 0 to 360^o. With increasing hue, color varies from red at 0^o, through green at 120^o, blue at 240^o, and back to red at 360^o. This is because the reflected color spectrum varies continuously from the longer wavelengths at red, to the shorter wavelengths towards blue.

3.2 Liquid Crystal Calibration

The primary purpose of calibration is to establish a relationship between the color displayed by the crystals and their respective temperatures. The color of scattered light recorded in the experiment depends on the viewing angle of the camera. For the choice of the LCT powder and camera position, the hue-angle relationship was found to be mostly linear with a slope equivalent to 0.07^{o}C per 10^o change of angle. The color-temperature calibration was conducted with the axes of the light source and camera remaining at right angles.

The calibration technique of the present study is essentially a point-wise routine for the entire illuminated plane in the beaker. In order to calibrate the color output of the liquid crystals, a series of images are recorded while the test section is at spatially uniform temperature. To create a uniform temperature environment, a circular copper plate of diameter equal to that of the beaker is positioned over a small volume of water, all other solid walls being maintained at constant temperature. At steady state, water is at a spatially uniform temperature. Consequently, the LCT image is nominally of uniform color, except for the possibility of noise. A series of 30 such images are recorded over the full range of temperatures considered in the study. These images are digitized into 8-bit color images, and subsequently converted to hue, saturation and intensity. A third order polynomial was found to be appropriate to fit the hue-temperature data.

4. Numerical Model

The images of the thermal field obtained using LCT are compared with the predictions of a numerical model (Banerjee and Muralidhar, 2005). The model assumes that the temperature and velocity fields are axisymmetric. In the presence of rotation, all three components of velocity are non-zero, though a function of the radial and vertical coordinates. The numerical model is based on a primitive variable formulation, previously discussed by Zhang and Prasad (1995). The approach adopted in the present study is presented in detail by Banerjee (2004). The code has been independently validated against other numerical solutions available in the literature. In addition, a careful grid independence study was carried out. A grid size of 80 × 80 has been used for an aspect ratio is unity, increasing proportionately for higher aspect ratios. The aspect ratio referred here is the ratio of depth of the water layer and the beaker radius. For the present simulation, the free surface is taken to be flat and thermo-capillary convection has been neglected. A convective-

radiative boundary condition is used at the free surface, with an effective heat transfer coefficient of 10 W/m^2K. The results reported in the following section are quite insensitive to this value. However, they respond strongly to the crucible-to-cylinder temperature difference and the cylinder rpm.

5. Results and Discussion

Experiments in the pure buoyancy regime, interaction of buoyancy with rotation, and validation against numerical simulation are described in the following sections.

5.1 Buoyancy-Driven Convection

Figures 2 and 3 show LCT images recorded in the experiments, with the inner cylinder held stationary. The temperature difference between the crucible and the inner cylinder sets up a natural convection current in the beaker. Several oscillations in the thermal pattern in the fluid were observed during the transient evolution of convection, particularly at higher temperature differences. After the passage of a sufficient amount of time, a stable, steady thermal field was attained, for every pair of hot and cold temperatures. It is interesting to note that colors revealed by LCT depend on the absolute temperatures employed in the experiment. However, the underlying flow patterns are sensitive to the temperature difference alone, and hence the Grashof number.

Under pure buoyancy conditions, the transfer of heat from the wall of the beaker lowers the density of water. As a result, water moves upwards along the beaker wall, while being cooled at the inner cylinder. The cold water being heavier descends along the axis of the beaker, setting up a counter-clockwise convection loop. Owing to a large difference in cross-sectional areas, the fluid velocities close to the beaker wall are small, while those near the axis are large. Thus, features such as plumes near the axis are better imaged in the present experimental setup.

In Figs. 2(a-c), the water bath used for maintaining constant temperature at the cylinder surface is set to a temperature of 34^oC, while the temperature of the second bath that maintains constant temperature conditions at the crucible wall is varied for each of the images. In Figs. 2(d-f), the temperature levels are changed, keeping the temperature difference a constant. As the average temperature of water in the beaker increases, the images proceed from red background to green, and ultimately show variations within the blue color. While any of these images is acceptable for quantitative analysis, Figs. 2(a) and 2(b) are the most suited for visualizing the thermal field.

Figure 2(a) shows that a red plume is formed along the axis of the crystal. The plume descending along the axis extends over the base of the beaker. The thickness of the plume decreases as it moves over the base of the beaker (indicating an increase in velocity), till it finally warms up and starts to rise along the beaker wall. For small temperature differences ($Gr = 1.07\times10^6$) the crucible contains a considerable amount of cold fluid, as seen by the red patches in Fig. 2(a). For higher temperature differences ($Gr = 2.13 \times 10^6$), the beaker is filled with warmer fluid of green color, the cold fluid being restricted to thin boundary layers, or within the plume, Fig. 2(c). Similar trends are seen in Figs. 2(d, e and f) where the crucible wall is set at higher temperature. The thermal field is seen to be practically axisymmetric for the range of temperatures used in the experiments of Fig. 2.

At a higher aspect ratio (Ar = 2) the plume thickness reduces, since the influence of the beaker wall temperature dominates convection. This result is seen in Figs. 3(a, b and c). The plume in essence starts as a cold jet from the cylinder surface, and becomes indistinguishable with the surrounding fluid a short distance later. The plume does not reach the base of the beaker, since it mixes with the warmer surrounding fluid first. On the other hand, at a very low aspect ratio, the increase in the thickness of the plume is pronounced, Figs. 3(d, e and f). Here, a roll that is formed fills the beaker volume. A special feature of the axisymmetric geometry is that fluid velocities in the vertical direction, near the axis tend to be large. The corresponding velocities near the beaker walls are smaller, due to a significant increase in cross-sectional area as well as wall friction. Thus, strong thermal plumes show up first near the axis, and the wall regions appear to be relatively passive.

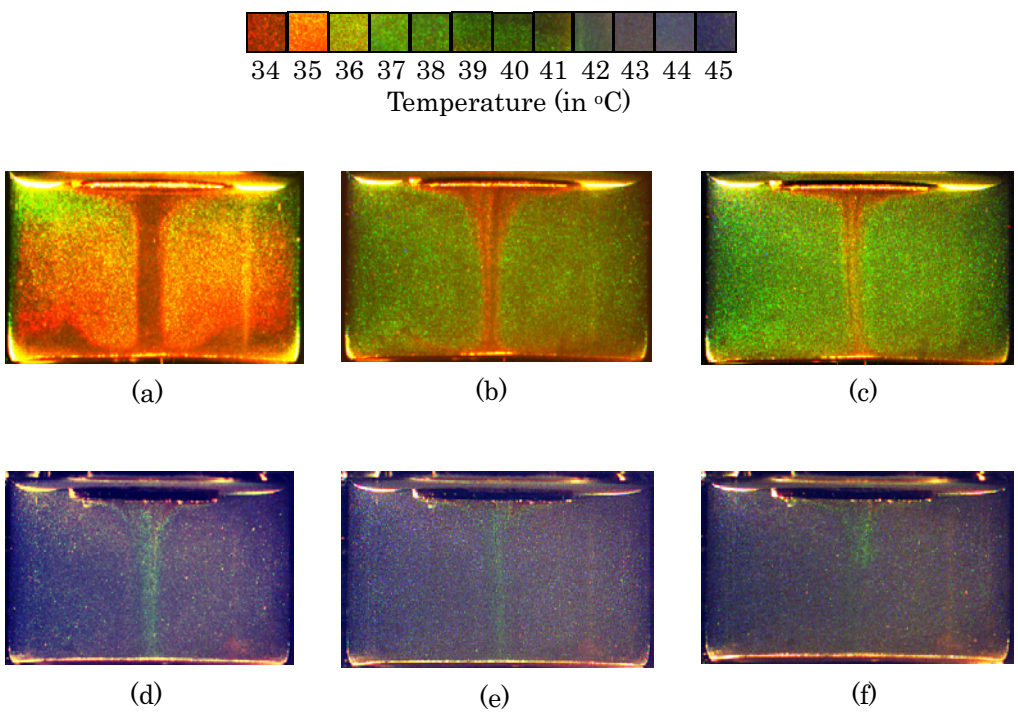

Fig. 2. LCT images of convection in the crucible without cylinder rotation for an aspect ratio of 1.0. The temperature of the cylinder surface and the crucible wall are: (a) 34°C and 36°C, Gr = 1.072 × 10^6; (b) 34°C and 37°C, Gr = 1.60 × 10^6; (c) 34°C and 38°C, Gr = 2.13 × 10^6; (d) 39°C and 45°C, Gr = 3.20 × 10^6; (e) 40°C and 45°C, Gr = 2.50 × 10^6; (f) 41°C and 45°C, Gr = 2.13 × 10^6.

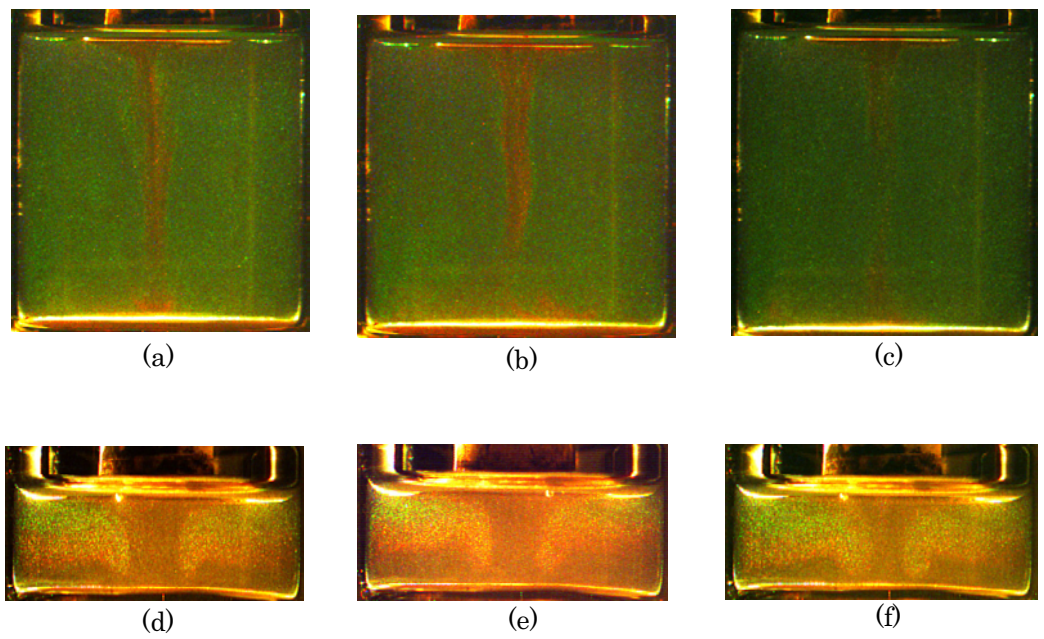

Fig. 3. LCT images of convection in the crucible without cylinder rotation for aspect ratios 2.0 (a, b, c) and 0.5 (d, e, f). The temperature of the cylinder surface and the crucible wall are: (a, d) 34°C and 36°C, Gr = 1.07 × 10^6; (b, e) 34°C and 37°C, Gr = 1.60 × 10^6; (c, f) 34°C and 38°C, Gr = 2.13 × 10^6.

5.2 Convection with Combined Buoyancy and Rotation

The convection patterns in the beaker at three different rotation rates (5, 15 and 25 rpm) are compared to those of natural convection in the sequence of images of Fig. 4. The temperatures of the two water baths are kept constant during the entire experiment at 34 and 36.5°C (Gr = 1.33 × 10^6). Owing to crystal rotation, a clockwise loop is formed closer to the axis, as the fluid particles move along the cylinder surface. This result is to be seen even at the lowest rotation rate. Closer to the beaker wall, a counter-clockwise roll driven by buoyancy is formed. With increasing rotation rate, the buoyancy-driven roll is further pushed towards the beaker wall, and is ultimately eliminated. The strength of the inner roll increases as the rotation rate increases. At the highest rotation rate, the thermal field is entirely determined by the rotational speed. The LCT images show that symmetry of the flow is preserved in the forced convection regime, but diminishes in the mixed convection regime (Figs. 4(b) and 4(c)). However, complete symmetry is seen in both the free and the forced convection regimes (Figs. 4(a) and 4(d)).

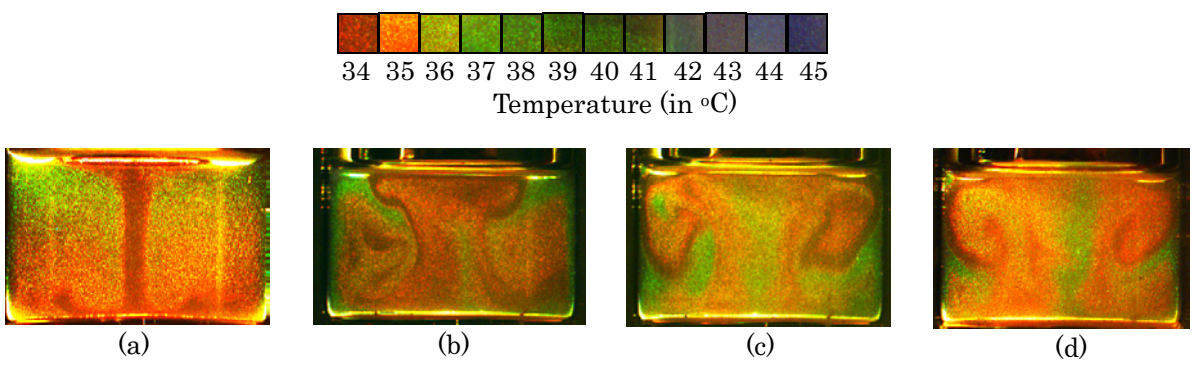

Fig. 4. LCT images of convection in the crucible with cylinder rotation for an aspect ratio of 1.0. The temperature of the crystal surface and the crucible wall are 34°C and 36.5°C, Gr = 1.33 × 10^6; rpm and rotational Reynolds number for different cases are (a) rpm = 0, Re = 0; (b) rpm = 5, Re = 0.65 × 10^3; (c) rpm = 15, Re = 1.95 × 10^3; (d) rpm = 25, Re = 3.25 × 10^3.

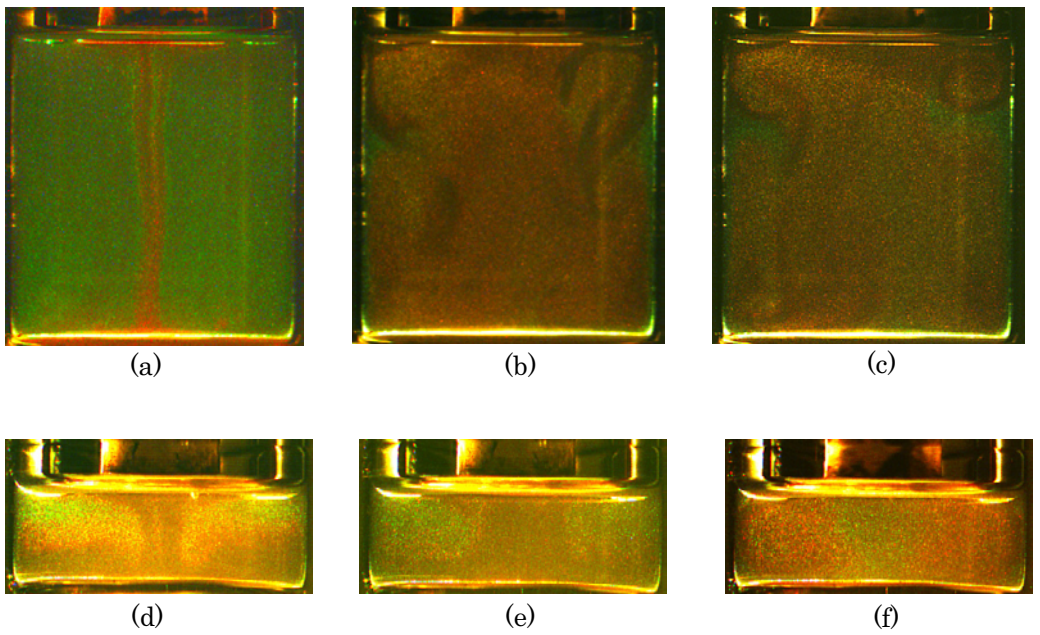

Fig. 5. LCT images of convection in the crucible with cylinder rotation for aspect ratios of 2 (a, b, c) and 0.5 (d, e, f). The temperature of the crystal surface and the crucible wall are 34°C and 36.5°C, Gr = 1.33 × 10^6; rpm and rotational Reynolds number for different cases are (a, d) rpm = 0, Re = 0; (b, e) rpm = 15, Re = 1.95 × 10^3; (c, f) rpm = 25, Re = 3.25 × 10^3.

The effect of rotation is presented for the high aspect ratio beaker (Ar = 2.0) in Figs. 5(a, b and c). In view of the large body of warm fluid in the beaker, the convection rolls are smaller and closer to the cylinder. However, the sequence proceeding from free, to mixed, to forced convection is once again observed. At a lower aspect ratio (Ar = 0.5), the entire fluid domain seems to be closer to an isothermal condition due to complete mixing of the flow by cylinder rotation, Figs. 5(a, b and c). Even in the mixed convection regime, the low aspect ratio experiments show symmetry in the circulation loops. The flow loops at the lower aspect ratio (Ar = 0.5) are more clearly defined, as compared to a higher aspect ratio (Ar = 2.0) beaker. The predominance of green color in the illuminated plane of the higher aspect ratio beaker shows that the beaker wall temperature has penetrated sufficiently into the fluid medium. The prominent appearance of red color in the lower aspect ratio beaker depicts strong cooling of the fluid by the copper cylinder. These results show that surface areas of the hot and cold walls play a role in determining the nature of convection. In dimensionless form, the relevant parameters are the aspect ratio and the radius ratio of the apparatus.

The S-shaped loops seen in Fig. 5(b) are indicative of chaotic conditions in the crucible and a loss of symmetry in the mixed convection regime of a high aspect ratio crucible. These trends were not seen for lower aspect ratio of 0.5, and the thermal field was visibly axisymmetric over the free, mixed and forced convection regimes.

5.3 Validation of the Numerical Code

The natural convection and forced convection images from the LCT experiments have been converted to data in the form of isotherms, and compared with numerical simulation, Fig. 6. While Re = 0 for natural convection, the highest rotation rate (Re = 3,250) has been chosen for the forced convection limit. The aspect ratio selected for comparison is unity. The two sets of results are seen to be in good agreement with one another. The direction of the convection rolls and the changes introduced by the effect of rotation are well reproduced in the simulation. In the intermediate range of rotation rates, the predictions of the numerical model were only in qualitative agreement with experiments. At the higher aspect ratio of 2, the differences were significant in the mixed convection regime, though the agreement between experiments and simulation was quite good at free and forced limits.

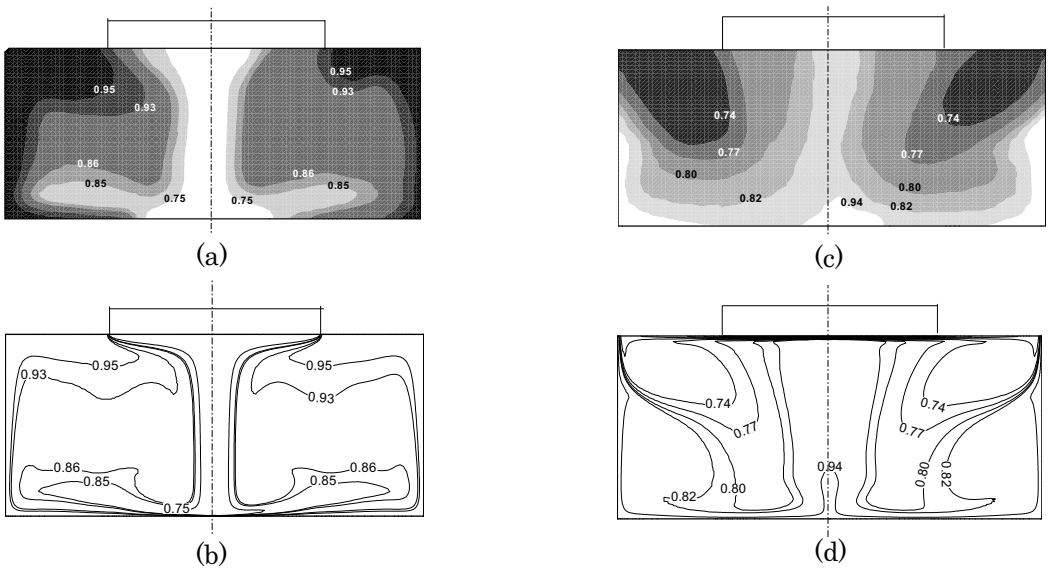

Fig. 6. Natural and forced convection in the crucible for aspect ratios 1.0. The temperature of the cylinder surface and the crucible wall are 34°C and 36.5°C, Gr = 1.33×10^6; rpm and rotational Reynolds number for different cases are (a, b) rpm = 0, Re = 0; (c, d) rpm = 25, Re = 3.25×10^3; (a, c) gray scale LCT images; (b, d) numerical isotherms based on an axisymmetric numerical model.

6. Conclusions

The temperature distribution in a model Czochralski crucible with water as the working fluid and a copper cylinder of smaller diameter placed above it was visualized using liquid crystal thermography. The following results have been obtained in the present study:

1. Buoyancy-driven convection shows axisymmetry for the range of temperature differences and aspect ratios considered.
2. The forced convection regime shows complete axisymmetry in the thermal field. The axisymmetry diminishes in the mixed convection regime. At higher aspect ratios, the flow becomes unsteady as well.
3. The natural and forced convection rolls are oppositely oriented.
4. Over the range of parameters studied, the experimental results for buoyant and forced convection are in good agreement with numerical simulation.

References

Banerjee, J., Czochralski growth of oxide crystals: Numerical simulation and experiments, Ph.D. dissertation, Indian Institute of Technology Kanpur, (2005).

Banerjee, J. and Muralidhar, K., Role of Internal Radiation during Czochralski Growth of YAG and Nd: YAG Crystals, International Journal of Thermal Sciences, (2005), Article in Press.

Derby, J. J. and Xiao, Q., Some effects of crystal rotation on large-scale Czochralski oxide growth: analysis via HTCM model, Journal of Crystal Growth, 113 (1991), 575-586.

Hintz, P. and Schwabe, D., Convection in a Czochralski Crucible, Part II: Rotating crystal, Journal of Crystal Growth, 222 (2001), 356-364.

Ireland, P. T. and Jones, T., V., Liquid crystal measurements of heat transfer and surface shear stress, Measurement Science Technology, 11 (2000), 969-986.

Jones, A. D. W., An experimental model of the flow in Czochralski growth, Journal of Crystal Growth, 61 (1983), 235-260.

Krishnamurti, R., On the transition to turbulent convection, Part I: Transition from two to three dimensional flow, Journal of Fluid Mechanics, 42-2 (1970), 295-307.

Mukherjee, D. K., Prasad, V., Dutta, P. and Yuan, T., Liquid crystal visualization of the effects of crucible and crystal rotation on Czochralski melt flows, Journal of Crystal Growth, 169 (1996), 136-146.

Szmyd, J. S. and Suzuki, K., Editors, Modeling and Transport Phenomena in Crystal Growth, (2000), WIT Press, London.

Zhang, H. and Prasad, V., A multizone adaptive process model for low and high pressure crystal growth, Journal of Crystal Growth, 155 (1995), 47-65.

Author Profile

Banerjee, Jyotirmay: He completed his doctoral thesis on "Czochralski Growth of Oxide Crystals: Numerical Simulation and Experiments" in the Department of Mechanical Engineering, IIT Kanpur (India) in January 2005. He is a lecturer in Mechanical Engineering at SVNIT, Surat (India).

Bharadwaj, R.: He is a doctoral student in the Department of Mechanical Engineering, SUNY, New York. Earlier he was a project associate at IIT Kanpur (India).

Muralidhar, K.: He is a Professor of Mechanical Engineering at IIT Kanpur (India). His research interests are in laser measurements, crystal growth, and transport phenomena in porous media.